5700 *Chem. Mater.* **2010,** *22,* 5700–5706
DOI:10.1021/cm101694g

CHEMISTRY OF MATERIALS
Article

Growth of RuO_2 Thin Films by Pulsed-Chemical Vapor Deposition Using RuO_4 Precursor and 5% H_2 Reduction Gas

Jeong Hwan Han,[†] Sang Woon Lee,[†] Seong Keun Kim,[†] Sora Han,[†] Cheol Seong Hwang,*[,†] Christian Dussarrat,[‡] and Julien Gatineau[‡]

[†]*WCU hybrid materials program, Department of Materials Science and Engineering and Inter-university Semiconductor Research Center, Seoul National University, Seoul 151-744, Korea, and* [‡]*Air Liquide, 28 Wadai, Tsukuba-Shi, Ibaraki Prefecture 300-4247, Japan*

Received June 17, 2010. Revised Manuscript Received August 16, 2010

RuO_2 thin films were grown on thermal SiO_2(100 nm) and Ta_2O_5(4 nm)/SiO_2(100 nm) substrates at 230 °C by pulsed-chemical vapor deposition using a RuO_4 precursor dissolved in blend of chosen organic solvent (with fluorinated solvents) and 95% N_2/5% H_2 mixed gas as the Ru precursor and reactant gas, respectively. The phase of the deposited film, either being RuO_2 or Ru, was controlled by the N_2/H_2 mixed gas feeding time. This was due to the fact that the time constant of the N_2/H_2 mixed gas for oxygen atom removal from the reaction surface was related to the reaction kinetics even under identical thermodynamic conditions. High-quality RuO_2 films could be deposited at the N_2/H_2 gas feeding time of 1−10 s, whereas a Ru film was grown with longer N_2/H_2 gas feeding times of >15 s. The saturated growth rate and resistivity of the RuO_2 thin films were 0.24 nm/cycle and ∼250 $\mu\Omega$ cm, respectively. Although the fundamental growth mechanism of the RuO_2 film was based on self-decomposition of the RuO_4 precursor, the N_2/H_2 reactant feeding served to enhance RuO_2 growth by the surface hydroxyl group-mediated chemisorption of the RuO_4 precursor. The RuO_2 film showed excellent step coverage inside a capacitor hole structure with an aspect ratio of 10 (opening diameter: 100 nm).

1. Introduction

Recently, noble metals, such as Ir, Pt, and Ru, have been studied extensively for electrodes of next generation dynamic random access memory (DRAM) capacitors with TiO_2-based high-*k* dielectric films, such as Al-doped TiO_2 and $SrTiO_3$ or (Ba,Sr)TiO_3.[1−9] Among the many electrode materials available, Ru and RuO_2 are promising materials because of their good susceptibility to dry etching, low resistivity (Ru, ∼7 $\mu\Omega$ cm; RuO_2, ∼30 $\mu\Omega$ cm), high chemical stability and high work function (Ru, ∼4.7 eV; RuO_2, 5.1 eV) compared to the currently used TiN electrode (∼4.2 eV). A high work function of the metal electrode is favorable for leakage current suppression because it increases the schottky barrier height at the metal−insulator junction of the capacitor. The rutile structure of RuO_2 films enables the local epitaxial growth of a rutile TiO_2 film with a high dielectric constant (80−130 from thin films[10,11]) even at a low growth temperature of 250 °C. The underlying layers in the integrated structure of a DRAM cell capacitor, such as the poly-Si plug or the TiN barrier, can be oxidized because of oxygen penetration during heat treatment. Therefore, electrode materials, such as Ru and RuO_2, which can block oxygen diffusion into the underlying layers, have been highlighted recently.[12] Moreover, it was reported that conducting oxide electrodes, such as RuO_2 and $SrRuO_3$, made less interfacial dead layers at the interface of the electrode/high-*k* dielectric film.[13]

The growth of RuO_2 films, either by metal−organic chemical vapor deposition (MOCVD) or atomic layer deposition (ALD), using MO precursors such as $Ru(EtCp)_2$ or $Ru(C_{11}H_{19}O_2)_3$ have been reported.[14−16] It was reported that the oxygen consumption by the metal−organic (MO)

*To whom correspondence should be addressed. E-mail: cheolsh@snu.ac.kr.

(1) Aaltonen, T.; Rahtu, A.; Ritala, M.; Leskelä, M. *Electrochem. Solid-State Lett.* **2003**, *6*, C130.
(2) Hwang, C. S.; Lee, B. T.; Kang, C. S.; Kim, J. W.; Lee, K. H.; Cho, H.-J.; Horii, H.; Kim, W.-D.; Lee, S. I.; Roh, Y. B.; Lee, M. Y. J. *Appl. Phys. Lett.* **1998**, *83*, 3703.
(3) Kim, S. K.; Lee, S. Y.; Lee, S. W.; Hwang, G. W.; Hwang, C. S.; Lee, J. W.; Jeong, J. *J. Electrochem. Soc.* **2007**, *154*, D95.
(4) Sun, H.-J.; Kim, Y.; Song, H.-S.; Lee, J.-M.; Roh, J.-S.; Sohn, H.-C. *Jpn. J. Appl. Phys.* **2004**, *43*, 1566.
(5) Lee, S. W.; Kwon, O. S.; Han, J. H.; Hwang, C. S. *Appl. Phys. Lett.* **2008**, *92*, 222903.
(6) Shibutami, T.; Kawano, K.; Oshima, N.; Yokoyama, S.; Funakubo, H. *Electrochem. Solid-State Lett.* **2003**, *6*, C117.
(7) Yoshikawa, K.; Kimura, T.; Noshiro, H.; Otani, S.; Yamada, M.; Furumura, Y. *Jpn. J. Appl. Phys.* **1994**, *33*, 867.
(8) Fröhlich, K.; ŤapaJna, M.; Rosová, A.; Dobročka, E.; Hušeková, K.; Aarik, J.; Aidla, A. *Electrochem. Solid-State Lett.* **2003**, *6*, C130.
(9) Kim, S.-W.; Kwon, S.-H.; Kwak, D.-K.; Kang, S.-W. *J. Appl. Phys.* **2008**, *103*, 023517.
(10) Kim, S. K.; Lee, S. Y.; Seo, M.; Choi, G.-J.; Hwang, C. S. *J. Appl. Phys.* **2007**, *102*, 024109.
(11) Choi, G.-J.; Kim, S. K.; Lee, S. Y.; Park, W. Y.; Seo, M.; Choi, B. J.; Hwang, C. S. *J. Electrochem. Soc.* **2009**, *156*, G71.
(12) Song, J.; Kim, H. R.; Park, J.; Jeong, S.; Hwang, C. S. *J. Mater. Res.* **2002**, *17*, 1789.
(13) Hwang, C. S. *J. Appl. Phys.* **2002**, *92*, 432.
(14) Rignanese, G.-M.; Gonze, X.; Jun, G.; Cho, K.; Pasquarello, A. *Phys. Rev. B* **2004**, *69*, 184301.
(15) Takagi, T.; Oizuki, I.; Kobayashi, I.; Okada, M. *Jpn. J. Appl. Phys.* **1995**, *34*, 4104.
(16) Kim, J.-H.; Kil, D.-S.; Yeom, S.-J.; Roh, J.-S.; Kwak, N.-J.; Kim, J.-W. *Appl. Phys. Lett.* **2007**, *91*, 052908.

Published on Web 09/28/2010

ligands at the surface and subsurface hinders sufficient oxidation of the adsorbed Ru atoms due to the higher oxidation potential of the MO ligands. Therefore, process modification or elongated feeding times of oxygen in the RuO_2 ALD (or MOCVD) process is necessary. Kim et al.[16] and Kang et al.[14] also reported that a high oxygen partial pressure promotes the growth of RuO_2 in the modified ALD (or MOCVD) process.

On the other hand, RuO_4, the Ru precursor used in this study, is a very strong oxidizer and is apt to decompose to form RuO_2 at low temperatures, even ~150 °C.[17] Therefore using this precursor to deposit RuO_2 films via properly controlled thermal decomposition(with the assistance of reducing agents) would be a more promising way to fabricate electrodes compared to the conventional method that utilizes the oxidative route of MO precursors and oxidizing reactants. The authors previously reported that high-quality Ru films could be grown with a low impurity concentration, high thermal stability, sufficient conformality, and high growth rate by pulsed-CVD (p-CVD) using RuO_4 as the Ru-precursor and a N_2/H_2 mixed gas as the reducing reactant.[18] In this study, the RuO_4 precursor and a 95% N_2/5% H_2 reducing gas were used to grow RuO_2 by controlling the N_2/H_2 mixed gas feeding time ($t_{N/H}$). In addition, by modifying the process sequences using an interrupted O_2 pulse, the growth mechanism of the RuO_2 and Ru thin films were examined.

2. Experimental Section

RuO_2 (or Ru) films were grown on thermally grown SiO_2 (100 nm) and Ta_2O_5 (4 nm)/SiO_2 (100 nm) substrates at 230 °C using a p-CVD method. The process module was an 8-in. diameter wafer scale shower-head type chamber (Quros Co., Plus-200). The RuO_4 was dissolved in a blend of chosen organic solvent, some having been fluorinated (ToRuS, produced by Air Liquide Co., with a density of 1.6 M). No carrier gas was used to deliver the precursor and the precursor solution was cooled to 3 °C to control its high vapor pressure (10 Torr at 25 °C). Details on ToRuS are reported elsewhere.[18,19] The N_2/H_2 mixed gas, which contained 5% H_2 in a N_2 background, was used as the reducing reactant. The chamber wall, showerhead, and precursor delivery line temperature were maintained at 50 °C. The p-CVD process consisted of a ToRuS pulse (1 s)−Ar purge (7 s)−reactant pulse (1−20 s)−Ar purge (5 s). The Ar purge gas flow rate was fixed to 600 standard cubic centimeters per minute (sccm). The N_2/H_2 mixed gas flow rate was fixed to 100 sccm. The working pressure was varied from 0.5 to 1.9 Torr. The Ta_2O_5 substrate film was grown by an MOCVD method using $Ta(OC_2H_5)_5$ [Pentakis (ethoxy) Tantalum] and O_2 as the Ta precursor and reactant, respectively, at 460 °C. The conformality of the RuO_2 films deposited on a three-dimensional hole structure, which was covered previously by a thermal ALD TiO_2 (4 nm thick) nucleation enhancing layer, was observed by scanning electron microscopy (SEM). The ALD TiO_2 layer was deposited on the hole structure using $Ti(i\text{-}OC_3H_7)_4$ and ozone gas as the Ti-precursor and oxygen source, respectively.[10] The crystallographic structure of the deposited films was examined by X-ray diffraction (XRD, PANalytical, X'pert Pro) in $\theta-2\theta$ mode. The film thickness and density of RuO_2 were analyzed by X- ray reflectivity (XRR), and the layer density of the deposited Ru atom was determined by X-ray fluorescence spectroscopy (XRF Themoscientific, ARL Quant'X). The chemical binding state of the Ruthenium 3d orbital was examined by X-ray photoelectron spectroscopy (XPS, KRATOS, AXIS-HSi). The depth profile of the chemical composition was examined by Auger electron spectroscopy (AES, Perkin-Elmer, Model 660). The morphology and root-mean-squared (rms) roughness of the RuO_2 film deposited on the Ta_2O_5 substrate were confirmed by SEM (Hitachi, S-4800) and atomic force microscopy (AFM, JSPM-5200). The sheet resistance of the deposited film was measured using a 4-point probe, and the film resistivity was calculated from the sheet resistance and film thickness.

3. Results and Discussions

The change in the Ru layer density according to RuO_4 pulse time was examined to verify whether the films were grown in ALD mode. However, no self-limiting saturation behavior was observed in all the $t_{N/H}$ regions tested because of thermal decomposition of the RuO_4 precursor at the growth temperature (230 °C).[18] The Ru layer density increased linearly with increasing RuO_4 feeding time, suggesting that ALD does not occur. (data not shown) Meanwhile, an interesting saturation behavior of the deposited Ru layer density with respect to the $t_{N/H}$ was observed. Figure 1a shows the change in Ru layer density as a function of $t_{N/H}$ (1 − 20 s) on the Ta_2O_5 substrate when other process parameters were fixed. The number of process cycles was 90 in all cases. The Ru layer density increased with increasing $t_{N/H}$ and approached the first saturation regime with a saturation layer density of ~12 $\mu g/cm^2$ at $t_{N/H}$ = 3−10 s. A further increase in $t_{N/H}$ resulted in a second saturation regime (saturation layer density of ~18 $\mu g/cm^2$) at $t_{N/H}$ > 15 s. The high Ru layer density at relatively long $t_{N/H}$ (> 10 s) could be explained by efficient reactions between the RuO_4 precursor and surface formed at such long $t_{N/H}$. In contrast, the saturated Ru layer density at $t_{N/H}$ = 3−10 s was ~60% of the film from the second saturation regime. This abrupt decrease in Ru layer density might result from the relatively inactive reaction between the RuO_4 precursor molecule and film surface, which was formed during the shorter $t_{N/H}$ (3−10 s) pulse. The origin of this 2-step saturation behavior will be discussed in detail later.

The resistivity and density of the films were examined to identify the phase of the films grown in the two saturation regions. Figure 1 (b) shows the changes in the resistivity and film density as a function of $t_{N/H}$. There is a critical point of $t_{N/H}$ between 10 and 15 s where the film resistivity and density change abruptly. The resistivity of the grown film was ~250 $\mu\Omega$ cm, which is higher than bulk value of RuO_2 (~ 35 $\mu\Omega$ cm)[20] when $t_{N/H}$ was < 10 s, and decreased to ~25 $\mu\Omega$ cm when $t_{N/H}$ was > 15 s. The film density was ~6.9 g/cm^3, which is close to the RuO_2

(17) Yuan, Z.; Puddepahtt, R. *Chem. Mater.* **1993**, *5*, 908.
(18) Han, J. H.; Lee, S. W.; Choi, G.-J.; Lee, S. Y.; Hwang, C. S.; Dussarrat, C.; Gatineau, J. *Chem. Mater.* **2009**, *21*, 207.
(19) Gatineau, J.; Yanagita, K.; Dussarrat, C. *Microelectron. Eng.* **2006**, *83*, 2248.
(20) Ryden, W. D.; Lawson, A. W.; Sartain, C. C. *Phys. Rev. B.* **1970**, *1*, 1494.

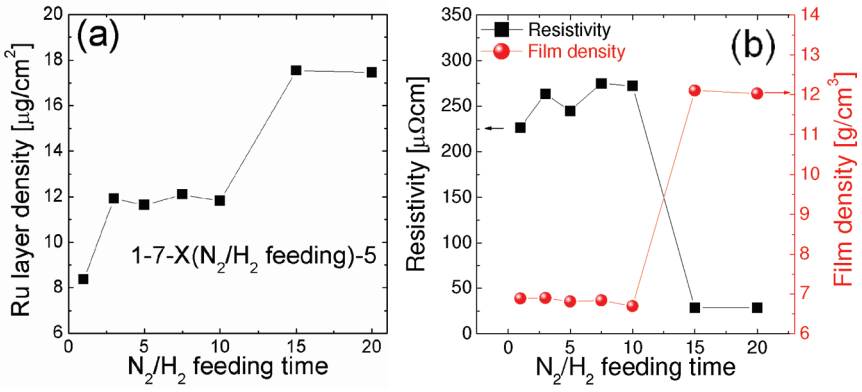

Figure 1. (a) Change in the Ru layer density on a Ta_2O_5 substrate as a function of the N_2/H_2 feeding time, (b) change in the resistivity and film density on Ta_2O_5 substrate as a function of the N_2/H_2 feeding time.

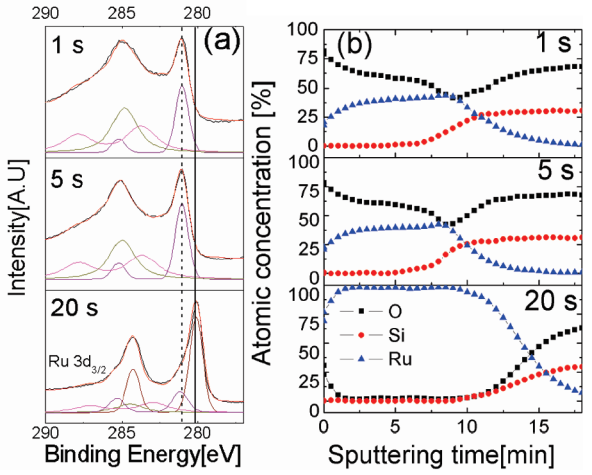

Figure 2. (a) Ru $3d_{5/2}$ XPS spectra of Ru and RuO_2 films with various N_2/H_2 gas feeding times ranging from 1 to 20 s, (b) AES depth profile of Ru and RuO_2 films with various N_2/H_2 gas feeding times.

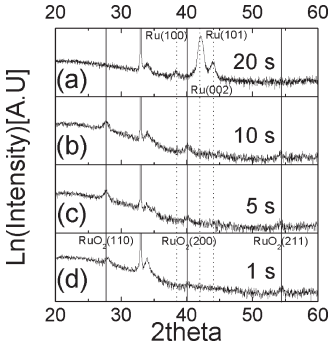

Figure 3. (a–d) The XRD patterns in $\theta-2\theta$ mode of the as grown film with different N_2/H_2 gas feeding times ranging from 1 to 20 s.

bulk density (7.026 g/cm^3) when the $t_{N/H}$ was <10 s, and increased to ~12.1 g/cm^3, which is close to that of bulk Ru (12.363 g/cm^3) when the $t_{N/H} > 15$ s. XPS and AES analyses were used to examine the chemical structure of the films depending on $t_{N/H}$. Figure 2a shows the Ru 3d XPS spectra of the deposited films with a $t_{N/H}$ of 1, 5, and 20 s grown on a thermal SiO_2 substrate. Also shown in Figure 2a are the deconvoluted spectra of the Ru $3d_{3/2}$ peak. The XPS peak positions were calibrated using the substrate Si 2p peak in SiO_2 (Si–O bonding, 103.3 eV) because the C1s peak overlaps with the peak position of Ru 3d (C 1s:285.0 eV, Ru $3d_{3/2}$:284.0 eV). When $t_{N/H} = 1$ and 5 s, the peak position of Ru $3d_{5/2}$ was located at ~281.2 eV, which corresponds to the binding energy of Ru $3d_{5/2}$ in RuO_2.[21] There was almost no Ru 3d peak at ~280 eV, which corresponds to metallic Ru, indicating that the film is composed of almost entirely RuO_2. On the other hand, the Ru $3d_{5/2}$ peak was clearly shifted to a lower binding energy at $t_{N/H} = 20$ s, suggesting that the film is mainly Ru. The deconvolution of the peaks shows that there is a small Ru $3d_{5/2}$ peak located at 281.2 eV. However, the intensity of this component peak was much smaller than those shown in the samples with $t_{N/H} = 1$ and 5 s. Figure 2b shows the corresponding AES depth profiles of the films grown on a SiO_2 substrate. The film contains 1–2% oxygen at $t_{N/H} = 20$ s (lower panel) suggesting that a metallic Ru film was deposited under these conditions. The oxygen concentration increased to ~60% when $t_{N/H} = 1$ and 5 s, indicating that a RuO_2 phase was grown under these conditions. These AES results are consistent with XPS analyses, which demonstrate that $t_{N/H}$ is one of the critical factors that determine the phase of the film. Similar AES results were obtained from the films on other substrates. (data not shown) The crystalline structure of the deposited film was examined by XRD. Figure 3a–d shows XRD patterns of the ~21 nm thick films when the $t_{N/H}$ values were 1, 5, 10, and 20 s, respectively. All the deposited films crystallized without post annealing. The diffraction peaks indicate that crystalline RuO_2 with a rutile structure [(110) at 28.03°, (200) at 40.05°, and (211) at 54.29°] was achieved when $t_{N/H}$ was <10 s as shown in Figure 3b–d. In contrast, Ru peaks were detected [(100) at 38.38°, (002) at 42.15°, and (101) at 44.00°] when $t_{N/H} = 20$ s, as shown in Figure 3a. The XRD results are also in agreement with the XPS and AES results shown in panels a and b in Figure 2. The above-mentioned analysis regarding the film composition and phase show that the film (also the growing film surface) changed abruptly from RuO_2 to Ru metal when $t_{N/H}$ was increased to 10–15 s.

(21) Madhavaram, H.; Idriss, H.; Wendt, S.; Kim, Y. D.; Knapp, M.; Over, H.; Assmann, J.; Löffler, E.; Muhler, M. *J. Catal.* **2001**, *202*, 296.

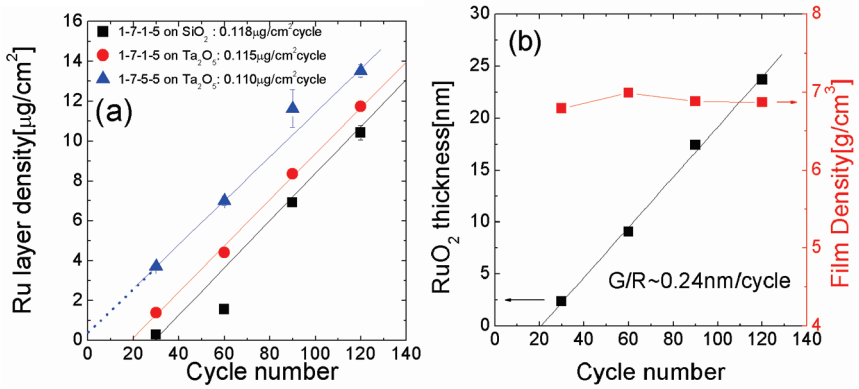

Figure 4. (a) Change in the Ru layer density on a SiO_2 and Ta_2O_5 substrate with 1−7−1−5 and 1−7−5−5 sequences as a function of the number of cycles. Here, numbers indicate the precursor, purge gas and N_2/H_2 gas pulse time. (b) Change in the thickness and density of RuO_2 film grown on Ta_2O_5 as a function of cycle number in case of $t_{N/H} = 1$.

Kang et al. reported that in CVD, when a MO precursor was used as the Ru precursor and O_2 was used as the oxidant, the phase of Ru or RuO_2 was determined by thermodynamic conditions, such as deposition temperature and oxygen partial pressure.[14] Kim et al. also reported that the phase of Ir or IrO_2 films deposited by ALD is controlled by the oxygen partial pressure and process temperature.[9] On the other hand, in this study, all factors except for the $t_{N/H}$ were fixed, and the $t_{N/H}$ in the adopted range could not affect the thermodynamic conditions during the process. Despite the identical thermodynamic conditions (temperature and oxygen partial pressure), the phase formation (RuO_2 or Ru) was determined by the $t_{N/H}$, which reveals that RuO_4 decomposition kinetics have a crucial role in the growth of the film. The reaction byproduct must be H_2O or −OH considering the reaction mechanism. The growth of a Ru film with a sufficient $t_{N/H}$ was reported elsewhere.[18] However, the formation of a RuO_2 phase using a shorter $t_{H/N}$ has not been reported.

Figure 4a shows the change in Ru layer density according to cycle number when the $t_{N/H} = 1$ and 5 s on the Ta_2O_5 substrates. For comparison, data for the SiO_2 substrate were also included when the $t_{N/H}$ was 1 s. The slope of the best-linear fitted lines were almost identical within experimental error range (0.11−0.12 $\mu g/cm^2 \cdot$cycle) irrespective of $t_{N/H}$ and type of substrate. This shows that the $t_{N/H}$ of 1 s is already long enough to grow RuO_2 films with a steady state growth rate. Although the $t_{N/H}$ does not affect the steady-state growth rate of the RuO_2 film significantly, it affects the initial growth behavior of the RuO_2 films. With a $t_{N/H} = 1$ s, the incubation cycle number for RuO_2 formation was approximately 20 on the Ta_2O_5 substrate (x-intercept), whereas almost no incubation period was observed in the case of $t_{N/H}$ of 5 s. This suggests that H_2 enhances film nucleation on the Ta_2O_5 substrate at the initial growth stage. On SiO_2 substrates, the number of incubation cycles was ~30, which is due to either the smaller amount of electron charge transfer from the SiO_2 substrate to the adsorbed precursor or the more covalent-like bonding properties of SiO_2.[21−23] Figure 4b shows changes in RuO_2 thickness and film density as a function of cycle number in the case of $t_{N/H} = 1$ when grown on a Ta_2O_5 substrate. Thickness and film density were analyzed by XRR measurements. The growth rate of the RuO_2 film was ~0.24 nm/cycle. The high density of the film in the low $t_{N/H}$ range was maintained down to a thickness of ~2.5 nm.

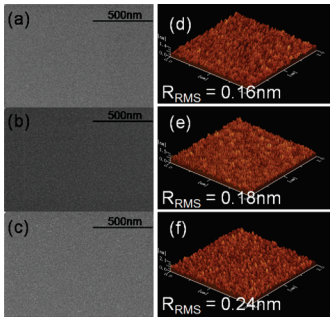

Figure 5. (a−c) SEM, an (d − f) AFM images of RuO_2 films deposited on Ta_2O_5 substrates with various cycle number at $t_{N/H} = 5$ s [(a, d) 30 cycles, (b, e) 60 cycles, (c, f) 90 cycles].

Figure 5a−c and d−f show the SEM plane view and AFM topographic images of the RuO_2 films grown on Ta_2O_5 at a $t_{N/H}$ of 5 s with a cycle number of: (a, d) 30, (b, e) 60, and (c, f) 90. Considering the growth rate of RuO_2, the film thickness was 7.2−21.6 nm. The RuO_2 films showed a very smooth surface morphology and the rms roughness was only ~0.2 nm at all cycle numbers, indicating the fluent nucleation behavior of RuO_2 on the substrate.

The saturated growth rate of the RuO_2 and Ru layer with respect to $t_{N/H}$ at different $t_{N/H}$ ranges is discussed below based on the surface-catalyzed thermal decomposition of the RuO_4 precursor. The authors recently reported that the growth of Ru metal films using the same precursor and reduction gas showed a CVD-like reaction in the Arrhenius type plot of growth rate over the temperature range of 180 to 350 °C.[18] Yuan et al. reported that thermal decomposition of the RuO_4 precursor produces

(22) Choi, B. J.; Choi, S.; Eom, T.; Ryu, S. W.; Cho, D.-Y.; Heo, J.; Kim, H. J.; Hwang, C. S.; Kim, Y. J.; Hong, S. K. *Chem. Mater.* **2009**, *21*, 2386.

(23) Kim, S. K.; Han, J. H.; Kim, G. H.; Hwang, C. S. *Chem. Mater.* **2010**, *22*, 2850.

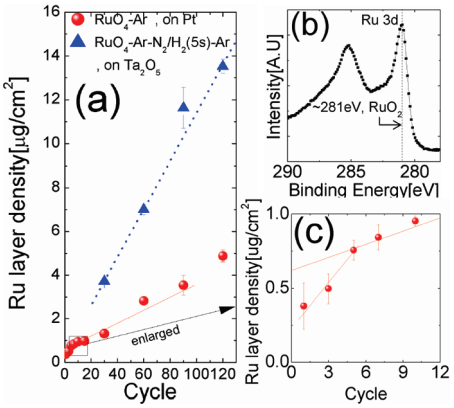

Figure 6. (a) Ru layer density of the deposited RuO_2 film with and without a N_2/H_2 feed on Ta_2O_5 (shown in Figure 1a) and Pt substrates, respectively, at 230 °C [triangle symbol: 1−7−5−5, 90 cycles, circle symbol: 1−7, 90 cycles], (b) XPS spectra of Ru 3d peak deposited without N_2/H_2 feeding on Pt, (c) enlarged plot of Figure 6 a for the Pt substrate.

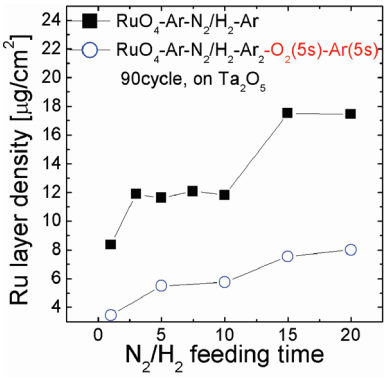

Figure 7. Change in Ru layer density as a function of the N_2/H_2 feeding time on Ta_2O_5 substrates with and without the additional O_2 pulse/purge steps.

RuO_2 with the formation of O_2 as a byproduct at temperatures <200 °C via a simple thermal decomposition reaction, as shown in eq 1.[17]

$$RuO_4 \rightarrow RuO_2 + O_2 \quad (1)$$

In this experiment, the H_2 gas may enhance RuO_2 growth through its reducing activity in addition to the thermal decomposition of the RuO_4 precursor described in eq 1. To confirm this, we attempted to grow the RuO_2 film by ToRuS feeding for 1 s followed by a 7 s Ar purge on a Pt substrate at the same growth temperature without subsequent N_2/H_2 gas feeding. For this experiment, Pt substrates were used instead of a Ru film in order to detect the amount of the adsorbed Ru atoms during steady state growth. Injection of the RuO_4 precursor on the Pt substrates is representative of the growth of Ru films at a steady growth stage because Pt can dissociate molecular oxygen to atomic oxygen like Ru due to its catalytic effect. Figure 6 (a) shows the change in Ru layer density as a function of cycle number on a Pt substrate (circle symbol). The figure also shows the data from the normal p-CVD RuO_2 (with N_2/H_2 pulse) on a Ta_2O_5 substrate for comparison, which were reproduced from data in Figure 4. The Ru layer density increased with increasing number of cycles on the Pt substrate even without reducing gas injection suggesting that the RuO_4 precursor is thermally decomposed at this temperature. Figure 6b shows the XPS spectra of the Ru 3d peak from the film deposited on a Pt substrate. The binding energy (281.0 eV) corresponds to the oxidized state in the form of RuO_2 suggesting that the deposited film was RuO_2. Interestingly, a faster growth rate (0.10 $\mu g/cm^2 \cdot$cycle) was achieved during the initial 5 cycles, as shown in Figure 6c. The growth rate of the Ru layer density decreased to 0.03 $\mu g/cm^2$ cycle after 5 cycles. It should be noted that the reaction surface was changed from Pt to RuO_2 after several growth cycles. Therefore, this result indicates that the Pt surface enhances the chemisorption and decomposition of RuO_4 molecules compared to RuO_2. This also appears to be the case for the Ru surface, as will be shown later. Figure 6a shows that the addition of a N_2/H_2 gas feeding step after the RuO_4 pulse step increases the saturated growth rate from 0.03 to 0.11 $\mu g/(cm^2$ cycle). This clearly shows that H_2 plays a key role in enhancing the growth rate of the RuO_2 layer by its strong reducing activity with RuO_4. This provides a clue to understanding the saturated growth rate of RuO_2 in the $t_{N/H}$ range from 3 to 10 s.

Wang et al. reported that H_2 molecules adsorb as water-like dihydride (H−O−H) on RuO_2 (110) surface at low temperatures.[24] When the temperature increases to above 350 K, it transforms to an energetically stable hydroxyl group (monohydride) at the bridging O site. This stable hydroxyl group might work as a favorable reaction center for the chemisorption of RuO_4 molecules during the subsequent RuO_4 pulse step. When hydrogen gas is injected, the RuO_2 surface is saturated with hydroxyl groups, as in the ALD of several oxides, and saturated RuO_4 adsorption can be achieved up to the $t_{N/H}$ of 10 s. Here, the supplied hydrogen atoms combine with the oxygen ions on the RuO_2 surface producing the hydroxyl groups. Sun et al. also reported that dissociated H_2 on the bridged oxygen site in the form of a hydroxyl group affects the surface electron density distribution.[25] Because of the polar nature of the hydroxyl group ($O^{\delta-}H^{\delta+}$) on the surface, the highly oxidative and electronegative RuO_4, which is as active as atomic oxygen,[26] is more likely to react with an OH-containing RuO_2 surface than a RuO_2 surface.

The growth mechanism and reason for the saturated growth of a Ru film with respect to $t_{N/H}$, when it is >15 s, is discussed. There are several reports on the reduction kinetics of noble metal oxides using a H_2 reducing agent[27,28] which can be a relevant guide to understanding metallic film growth. According to these reports, a relatively long induction time is needed to reduce a noble metal oxide (such as RuO_2 and Rh_2O_3) to a metal phase in a H_2 atmosphere. Williams et al.[27] reported that during the induction time,

(24) Wang, J.; Fan, C. Y.; Sun, Q.; Reuter, K.; Jacobi, K.; Scheffler, M.; Ertl, G. *Angew. Chem.* **2003**, *115*, 2201.
(25) Sun, Q.; Reuter, K.; Scheffler, M. *Phys. Rev. B.* **2004**, *70*, 235402.
(26) Moro-oka, Y. *Catalysis Today*. **1998**, *45*, 3.
(27) Williams, C. T.; Chen, E. K.-Y.; Takoudis, C. G.; Weaver, M. J. *J. Phys. Chem.* **1998**, *102*, 4785.
(28) Prudenziati, M.; Morten, B.; Travan, E. *Mater. Sci. Eng.* **2003**, *B98*, 167.

Table I. Chemical Equations of Ru and RuO_2 Deposition for Both RuO_4/H_2 Pulse and $RuO_4/H_2/O_2$ Pulse

	$t_{N/H} < 10$ s	$t_{N/H} > 15$ s
RuO_4/H_2 pulse	$RuO_2 \cdot H + RuO_4(g) \rightarrow 2RuO_2 + xH_2O(g)$ $RuO_2 + xH_2(g) \rightarrow RuO_2 \cdot H + yH_2(g)$	$Ru + RuO_4(g) \rightarrow 2RuO_2$ $RuO_2 + 2H_2(g) \rightarrow Ru + 2H_2O(g)$
$RuO_4/H_2/O_2$ pulse	$RuO_2 \cdot H + O_2(g) \rightarrow RuO_2 + xH_2O(g)$ further adsorption of RuO_4 on RuO_2 is retarded	$2Ru + O_2(g) \rightarrow Ru\text{-}RuO_2$*(surf) further adsorption of RuO_4 on RuO_2*(surf) is retarded

the reduction reaction does not occur despite the continuous H_2 feed. However, after the induction time has elapsed, rapid first-order reduction occurrs "auto catalytically". This "autocatalytic" reaction means that the reduction reaction can be strongly activated once the metallic material, which has a catalytic activity for oxide decomposition, is nucleated. Therefore, once a part of the growth surface changes from RuO_2 to Ru by a long $t_{N/H}$, the entire surface transforms rapidly to Ru by the autocatalytic reduction reaction.

Once the surface is transformed to a Ru surface, an even faster chemisorption of RuO_4 is expected from the disproportionation reaction shown in eq 2.[17]

$$RuO_4 + Ru \rightarrow 2RuO_2 \quad (2)$$

The disproportionation reaction may provide a CVD reaction with a further driving force for deposition. The Ru film grows with a higher growth rate because the $t_{N/H}$ is long enough to induce the reduction of RuO_2 to Ru and the autocatalytic reduction reaction, as shown in Figure 1a takes place under these conditions. The presence of a disproportionation reaction also explains the higher and saturated growth rate at $t_{N/H} > 15$ s. A certain saturated amount of RuO_4 is adsorbed chemically on the exposed Ru surface, of which the surface atomic density is fixed irrespective of the $t_{N/H}$.

The suggested growth mechanism for the RuO_2 and Ru film by the H_2 effect was further verified using an additional O_2 step after the p-CVD RuO_2 sequence [ToRuS pulse−Ar purge−N_2/H_2 pulse−Ar purge−O_2 pulse (5 s)−Ar purge (5 s)]. For this experiment, a Ta_2O_5 substrate was used and the total RuO_4 pulse number was fixed to 90.

Figure 7 shows the change in Ru layer density when the surface state of the deposited film was modified by the additional oxygen pulse steps. The results shown in Figure 1a were also included (solid square symbol) for comparison. The blank circle symbol, which shows the effect of additional oxygen treatment, shows that a significant decrease in the Ru layer density occurred when the film surface was treated with oxygen for both the RuO_2 and Ru films. This means that the chemisorption of the RuO_4 precursor was much less active on an oxidized film surface than on a hydroxyl-group-terminated surface. The surface OH-group density on the RuO_2 surface might be reduced by O_2 gas. This is consistent with the growth model that assumes the growth rate is determined mainly by the amount of RuO_4 chemisorption on the film surface. The state of the surface is determined by the gas pulse step immediately before the precursor pulse step. The phase of the films with an additional oxygen gas pulse sequence was the same as those without the additional oxygen gas at a given $t_{N/H}$. (data now shown) Chemical equations of deposition schemes for both cases of RuO_4/H_2 pulsing and $RuO_4/H_2/O_2$ pulsing when $t_{N/H} < 10$ s and $t_{N/H} > 15$ s are summarized in Table I.

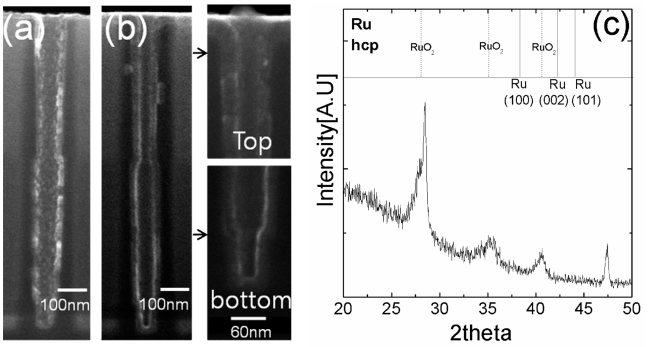

Figure 8. (a, b) Cross-section SEM image showing the three-dimensional conformality of the RuO_2 film on a capacitor hole structure formed in ALD TiO_2/SiO_2 with a opening diameter of 100 nm and a depth of 1000 nm [(a)1 s N_2/H_2 feeding, (b) 5 s N_2/H_2 feeding]; (c) the XRD pattern in $\theta-2\theta$ mode of the as grown film on a hole structure with 5 s N_2/H_2 gas feeding.

Sufficient step coverage of the RuO_2 film is crucial for the application of RuO_2 films as the electrode in DRAM capacitors with a three-dimensional structure. Images a and b in Figure 8 show SEM vertical cross-section images of a RuO_2 film grown for 120 cycles on a hole structure formed inside a SiO_2 layer with an aspect ratio of 10 and top opening diameter of ~100 nm. A 4 nm thick ALD TiO_2 layer was deposited previously to allow better nucleation of the RuO_2 layer. The RuO_2 film was deposited with a $t_{N/H}$ of 1 s (Figure 8a) and 5 s (Figure 8b). Although both samples shows that excellent step coverage (which means thickness ratio between the top and bottom corners, > 90%) was obtained (right panels of Figure 8b show the enlarged images of the film at the top and bottom corners), the RuO_2 film with $t_{N/H} = 5$ s showed a smoother film because of the shorter incubation period and accompanying better nucleation (Figure 4). Figure 8c shows the XRD θ-2θ scan data of the RuO_2 film on a capacitor hole structure, indicating that the entire film is composed of RuO_2. There was no diffraction peak for the Ru phase.

4. Conclusions

RuO_2 thin films were grown by pulsed-CVD using RuO_4 and 95% N_2/5% H_2 mixed gas as the Ru precursor and reducing reactant, respectively, at a growth temperature of 230 °C. In contrast to the previous attempts to grow RuO_2 films using MO precursors and an oxidative reactant, this study adopted an alternative route to synthesize RuO_2 via the kinetically limited reduction of RuO_4 by H_2. In addition to the generic thermal decomposition of the RuO_4 at the growth temperature, surface OH-group mediated chemical adsorption of the precursor on the RuO_2 surface made a significant contribution to RuO_2

film growth at relatively low N_2/H_2 gas pulse times (3−10 s). This surface OH-mediated growth also induced a saturated growth behavior with the N_2/H_2 gas pulse time. When the N_2/ H_2 gas pulse time was increased to more than a critical value (10−15 s), the RuO_2 abruptly reduced to Ru by the autocatalytic reduction effect of the Ru nuclei. On the Ru layer, film deposition was enhanced further by the disproportionation reaction between RuO_4 and Ru. The growth rate and density of the RuO_2 film was 0.24 nm/cycle and 6.9 g/cm^3, respectively. The resistivity of the RuO_2 thin film was ∼250 $\mu\Omega$ cm. On the capacitor hole structure of TiO_2 (4 nm)/SiO_2 with an aspect ratio of 10 (opening diameter is 100 nm), the RuO_2 film showed excellent step coverage. Longer N_2/H_2 gas pulse times were beneficial in obtaining a smoother surface morphology on the capacitor hole structure.

Acknowledgment. This work was partly supported by the IT R&D program of MKE/KEIT [KI002178, Development of a mass production compatible capacitor for next generation DRAM], the Converging Research Center Program through the National Research Foundation of Korea (NRF) funded by the Ministry of Education, Science and Technology (2009-0081961), and World Class University program through the Korea Science and Engineering Foundation funded by the Ministry of Education, Science and Technology (R31-2008-000-10075-0).